Manifestation of helical edge states as zero bias magneto-tunneling-conductance peaks in noncentrosymmetric superconductors

2009 J. Phys.: Condens. Matter 21 375702

(http://iopscience.iop.org/0953-8984/21/37/375702)

IOP PUBLISHING JOURNAL OF PHYSICS: CONDENSED MATTER

J. Phys.: Condens. Matter **21** (2009) 375702 (7pp) doi:10.1088/0953-8984/21/37/375702

Manifestation of helical edge states as zero bias magneto-tunneling-conductance peaks in noncentrosymmetric superconductors

Soumya P Mukherjee and Sudhansu S Mandal

Department of Theoretical Physics, Indian Association for the Cultivation of Science, Jadavpur, Kolkata 700 032, India

Received 2 July 2009
Published 19 August 2009
Online at stacks.iop.org/JPhysCM/21/375702

Abstract
Helical edge states exist in the mixed spin singlet and triplet phase of a noncentrosymmetric superconductor (NCSS) when the pair amplitude (PA) in the negative helicity band, Δ_-, is smaller than the PA in the positive helicity band, Δ_+, i.e., when the PA in the triplet component is more than the same in the singlet component. We numerically determine energies of these edge states as a function of $\gamma = \Delta_-/\Delta_+$. The presence of these edge states is reflected in the tunneling process from a normal metal to an NCSS across a bias energy eV. (i) Angle resolved spin conductance (SC) obeying the symmetry $g_s(\phi) = -g_s(-\phi)$ shows peaks when the bias energy equals the available quasiparticle edge state energy provided $|eV| \lesssim \Delta_-$. (ii) The total SC, G_s, is zero but modulates with eV for finite magnetic field H. (iii) The zero bias peaks of G_s and total charge conductance, G_c, at finite H split into two at finite eV for moderate H. (iv) At zero bias, G_c and G_s increase with H and show peaks at $|H| \sim \gamma H_0$, where H_0 is a characteristic field.

(Some figures in this article are in colour only in the electronic version)

1. Introduction

Recently discovered noncentrosymmetric (NCS) superconductors such as $CePt_3Si$ [1] and Li_2Pt_3B [2] having strong spin–orbit interaction (SOI) among various types of unconventional superconductors are of current interest in their own right. Besides superconductivity at the interfaces, such as the interface between $LaAlO_3/SrTiO_3$ [3], may also be classified as a two-dimensional NCS superconductivity due to the strong potential gradient. The SOI in NCS superconductors leads to a mixture of the spin singlet (s-wave) and triplet (p-wave) pairing [4]; the pairing amplitude in positive (negative) helicity band is Δ_+ (Δ_-) with $p_y - ip_x$ symmetry. The triplet pairing occurs in both $s_z = -1$ and $+1$ channels but their chiral p-wave symmetries are conjugate [5] to each other, where s_z is the spin component of a triplet pair along quantization direction. Thus, nonmagnetic NCS superconductors have the potential of producing spin current without magnetic field. These may produce a Josephson spin tunneling current [5] between two NCS superconductors and a spin tunneling current [7] due to Andreev reflection [6] across the junction between a normal metal and NCS superconductor. Both the up and the down spin holes will be reflected in the Andreev process; consequently a spin polarized tunneling current flows.

There exists a helical edge mode [7, 8] when the superconductor has more triplet components with $p_y \pm ip_x$ symmetry than singlet component. The low energy Andreev reflection is mostly due to these edge modes and the incident angle dependent spin polarized current flows [7] through the interface. In the presence of a magnetic field, the incident-angle-integrated current is also spin polarized. There is no helical edge mode for purely s-wave symmetry. The existence of zero energy Majorana fermions at the vortex state and their obeying non-Abelian statistics [9] is also a possibility in NCS superconductors [10] *a la* the chiral p-wave superconductor [11], such as Sr_2RuO_4 [12].

The helical edge state is present [7, 8] in NCS superconductors when the magnitude of the triplet component of the pair amplitude is larger than the singlet component, i.e., when the ratio between the pair amplitudes in negative and positive helicity bands, $\gamma = \Delta_-/\Delta_+ > 0, (\Delta_- < \Delta_+)$. Applying boundary condition at the edges, Tanaka *et al* [7] have found that the bound state energy E is proportional to transverse momentum k_y for small k_y. In this paper, we numerically obtain the energy of the edge states for all permissible k_y, since all of these have role in the tunneling process. We find that the midgap quasiparticle energy ($E < \Delta_-$) for the edge state decreases with γ.

Although the tunneling charge and spin conductances for *purely* triplet symmetry (i.e., for $\gamma = 1$) have been studied by Tanaka *et al* [7], exploration for the mixed triplet and singlet symmetries is necessary since in the system like Li_2Pt_3B, triplet and singlet components are comparable [2]. We employ the method of Tanaka *et al* [7] and study tunneling conductances for different proportionate mixture of triplet and singlet components ($\gamma \neq 1$) in this paper and find new and interesting consequences. The angle resolved spin current, denoted as $g_s(\phi)$, shows peaks at those values of incident angle ϕ for which the energy of the incident electron is equal to the quasiparticle bound state energy, provided the bias energy $|eV| \lesssim \Delta_-$, it obeys the symmetry $g_s(\phi) = -g_s(-\phi)$, and hence the total spin conductance G_s is zero at zero magnetic field. However, at finite magnetic field G_s is finite and obeys the symmetry $G_s(eV, H) = -G_s(-eV, H) = -G_s(eV, -H)$. The total charge conductance G_c shows a dip at the bias energy $|eV| = \Delta_-$, a zero bias peak (ZBP) at zero magnetic field, splitting of the peak into two at finite bias and a dip at zero bias for moderate magnetic field, and then the reappearance of the ZBP at higher magnetic field before it eventually vanishes at very high magnetic field. Although G_s is zero at zero magnetic field, it shows ZBP at finite magnetic field. The splitting and shifting of peaks at finite bias with the increase of magnetic field is similar as in the case of G_c. The magnitudes of both G_c and G_s at zero bias increase with $|H|$ and show peaks at $|H| \sim \gamma H_0$, with $H_0 = \Phi_0/(\pi^2\xi\lambda_d)$, which is the characteristic field where Φ_0 is the flux quantum, ξ is the coherence length and λ_d is the penetration length of the superconductor.

The paper is organized as follows. In section 2, we derive an equation for the quasiparticle energy of the helical edge state in a noncentrosymmetric superconductor using the boundary condition of forming bound states. This equation is numerically solved to find the energies of the quasiparticle bound states. The tunneling charge and spin conductances from a normal metal to a NCS superconductor in the absence and presence of a magnetic field are formulated in section 3. The conductances are numerically determined and the results are presented in section 4. We summarize our results in section 5.

2. Helical edge state

We begin with the Hamiltonian for an NCS superconductor in which Cooper pairs form between the electrons within the same spin-split band:

$$\mathcal{H} = \sum_{\mathbf{k},\lambda=\pm} [\xi_{\mathbf{k}\lambda} c^\dagger_{\mathbf{k}\lambda} c_{\mathbf{k}\lambda} + (\Delta_{\mathbf{k}\lambda} c^\dagger_{\mathbf{k}\lambda} c^\dagger_{-\mathbf{k}\lambda} + \text{h.c.})], \quad (1)$$

where $\xi_{\mathbf{k}\lambda} = \xi_{\mathbf{k}} + \lambda\alpha|\mathbf{k}|$ for Rashba SOI [13], $\xi_{\mathbf{k}} = \hbar^2\mathbf{k}^2/(2m) - \mu$. Here μ, m, λ, $\mathbf{k}$, α, and $\Delta_{\mathbf{k}\lambda}$ denote chemical potential, mass of an electron, spin-split band index ($\pm$), momentum of an electron, coupling constant of Rashba SOI given by $\hat{V}_{so} = \alpha\boldsymbol{\eta}_{\mathbf{k}} \cdot \hat{\boldsymbol{\sigma}}$ with $\boldsymbol{\eta}_{\mathbf{k}} = \hat{y}k_x - \hat{x}k_y$ and the Pauli matrices $\boldsymbol{\sigma}$, and pair potential in band λ respectively. We choose $k_y + \mathrm{i}k_x$-wave pair in both the bands, i.e., $\Delta_{\mathbf{k}\lambda} = \Delta_\lambda\Lambda_{\mathbf{k}}$ with $\Lambda_{\mathbf{k}} = -\mathrm{i}\exp[-\mathrm{i}\phi_{\mathbf{k}}]$. This corresponds to triplet component of pair potential $\hat{\Delta}_T = (\boldsymbol{d}_{\mathbf{k}} \cdot \boldsymbol{\sigma})\mathrm{i}\sigma_y$ with $\boldsymbol{d}_{\mathbf{k}} = \frac{1}{2|\mathbf{k}|}(\Delta_+ + \Delta_-)\boldsymbol{\eta}_{\mathbf{k}}$, i.e., the amplitude of the triplet component $\Delta_t = \frac{1}{2}(\Delta_+ + \Delta_-)$ and the singlet component of the pair potential is $\hat{\Delta}_S = \mathrm{i}\Delta_s\sigma_y$ with amplitude $\Delta_s = \frac{1}{2}(\Delta_+ - \Delta_-)$ [5]. Therefore the superconductor is purely triplet with $k_y + \mathrm{i}k_x$-wave symmetry when $\Delta_+ = \Delta_-$, purely singlet with s-wave symmetry when $\Delta_- = -\Delta_+$, and triplet and singlet components with equal amplitude when $\Delta_- = 0$. Therefore the Hamiltonian (1) in the matrix form [4] read as

$$H = \begin{pmatrix} \hat{h}_{\mathbf{k}} & \hat{\Delta}_{\mathbf{k}} \\ -\hat{\Delta}^*_{-\mathbf{k}} & -\hat{h}^*_{-\mathbf{k}} \end{pmatrix}, \quad (2)$$

where $\hat{h}_{\mathbf{k}} = \xi_{\mathbf{k}} + \hat{V}_{so}$ and $\hat{\Delta}_{\mathbf{k}} = \hat{\Delta}_T + \hat{\Delta}_S$. The solution of the Hamiltonian (2) in the bulk is with the energy eigenvalues $\pm\sqrt{\xi_+^2 + \Delta_+^2}$ and $\pm\sqrt{\xi_-^2 + \Delta_-^2}$, in line with the Cooper pairing between electrons within the same spin-split band. Correspondingly, there are two Fermi surfaces with Fermi momenta $k_F^\pm = \mp m\alpha/\hbar^2 + \sqrt{(m\alpha/\hbar^2)^2 + 2m\mu/\hbar^2}$, i.e., $k_F^+ < k_F^-$.

Consider a two-dimensional semi-infinite NCS superconductor with the edge along y-direction such that the edge is located at $x = 0$ and the superconductor is in the region $x > 0$. We then mix two quasiparticle and two quasihole states at and near the edge. The corresponding wavefunction will have the form

$$\Psi_S(x, y) = \mathrm{e}^{\mathrm{i}k_y y}[\mathrm{e}^{-\kappa_+ x}\{c_1\,\psi_e^+ \mathrm{e}^{\mathrm{i}k^+_{Fx}x} + c_2\,\psi_h^+ \mathrm{e}^{-\mathrm{i}k^+_{Fx}x}\} + \mathrm{e}^{-\kappa_- x}\{d_1\,\psi_e^- \mathrm{e}^{\mathrm{i}k^-_{Fx}x} + d_2\,\psi_h^- \mathrm{e}^{-\mathrm{i}k^-_{Fx}x}\}], \quad (3)$$

where Fermi momenta along x-direction in two spin-split bands are $k^\pm_{Fx} = \sqrt{k_F^{\pm 2} - k_y^2}$. Quasiparticle and quasihole wavefunctions [7] in two spin-split bands ($\pm$) are given by

$$\psi_e^+ = \begin{pmatrix} u_+ \\ -\mathrm{i}\mathrm{e}^{\mathrm{i}\phi_+}u_+ \\ \mathrm{i}\mathrm{e}^{\mathrm{i}\phi_+}v_+ \\ v_+ \end{pmatrix}, \qquad \psi_h^+ = \begin{pmatrix} v_+ \\ +\mathrm{i}\mathrm{e}^{-\mathrm{i}\phi_+}v_+ \\ -\mathrm{i}\mathrm{e}^{-\mathrm{i}\phi_+}u_+ \\ u_+ \end{pmatrix}, \quad (4)$$

$$\psi_e^- = \begin{pmatrix} u_- \\ \mathrm{i}\mathrm{e}^{\mathrm{i}\phi_-}u_- \\ \mathrm{i}\mathrm{e}^{\mathrm{i}\phi_-}v_- \\ -v_- \end{pmatrix}, \qquad \psi_h^- = \begin{pmatrix} v_- \\ -\mathrm{i}\mathrm{e}^{-\mathrm{i}\phi_-}v_- \\ -\mathrm{i}\mathrm{e}^{-\mathrm{i}\phi_-}u_- \\ -u_- \end{pmatrix}, \quad (5)$$

with $\frac{u_\pm}{v_\pm} = (E - \mathrm{i}\Gamma_+)/\Delta_+$, $\frac{u_-}{v_-} = (E - \mathrm{i}\Gamma_-)/\Delta_-$, and $\Gamma_\pm = \sqrt{\Delta_\pm^2 - E^2}$ for an edge state with energy E, and $\sin(\phi_\pm) = k_y/k_F^\pm$. Here c_1, c_2, d_1, and d_2 are the corresponding weights at which these four quasiparticle and quasihole states mix, and $\kappa_\pm = m\Gamma_\pm/k^\pm_{Fx}$ are the inverse of the length scales of localized edge states for the two spin-split bands.

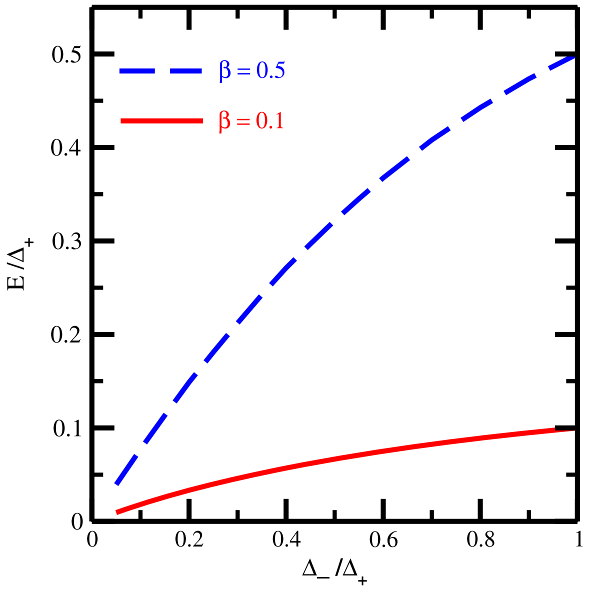

Figure 1. The variation of edge state energy of the quasiparticles with the ratio of pair amplitudes between two spin-split bands for $\beta = 0.5$ and 0.1. $E = \beta\Delta_+$ for $\Delta_-/\Delta_+ = 1$ and E converges towards zero for all values of Δ_-/Δ_+. However, $E = 0$ only for $\beta = 0$, i.e., $\phi_\pm = 0$.

The boundary condition $\Psi(x = 0, y) = 0$ determines the ratio between the coefficients a, b, c, and d and consequently we find an identity

$$\frac{(\frac{u_+}{v_+})(\frac{u_-}{v_-}) + 1}{\frac{u_+}{v_+} + \frac{u_-}{v_-}} = |\beta| = \left|\frac{\sin[\frac{1}{2}(\phi_+ + \phi_-)]}{\cos[\frac{1}{2}(\phi_+ - \phi_-)]}\right|. \qquad (6)$$

Putting expressions of u_+/v_+ and u_-/v_- in equation (6), we find

$$E^2 + \Delta_+\Delta_- - \Gamma_+\Gamma_- - \mathrm{i}E(\Gamma_+ + \Gamma_-) = |\beta|[E(\Delta_- + \Delta_+) - \mathrm{i}(\Delta_-\Gamma_+ + \Delta_+\Gamma_-)] \qquad (7)$$

for positive energy quasiparticles. An equivalent equation for edge state energy is also derived in [7]. For a purely triplet superconductor, i.e., for $\Delta_+ = \Delta_-$, $E = |\beta|\Delta_+$. The solution of equation (7) as a function $\gamma = \Delta_-/\Delta_+$ for $\beta = 0.5, 0.1$ is shown in figure 1. The zero energy edge state is possible only for $\beta = 0$ for all $\Delta_-/\Delta_+ > 0$, $(\Delta_- < \Delta_+)$. There is no edge state for $\Delta_- = 0$, i.e., when the triplet amplitude and singlet amplitude will be of equal magnitude. This is because the superconductivity exists only in the band of positive helicity as the negative helicity band becomes normal in this case. If $E = \Delta_-$, $u_- = v_-$ and consequently $\beta = \pm 1$ which suggests $|\phi_+| = \pi/2$.

When $\Delta_t < \Delta_s$, the pair amplitude in the negative helicity band is negative ($\Delta_- < 0$). In that case the signs of the third and fourth components of ψ_e^- and ψ_h^- in equation (5) change. Therefore equation (7) in this case reduces to

$$E^2 + \Delta_+\Delta_- - \Gamma_+\Gamma_- - \mathrm{i}E(\Gamma_+ + \Gamma_-) = |\beta|[-E(\Delta_+ + \Delta_-) + \mathrm{i}(\Delta_-\Gamma_+ + \Delta_+\Gamma_-)]. \qquad (8)$$

This equation does not produce any solution in the range $\Delta_- \leqslant E \leqslant -\Delta_-$ except when the magnitudes of Δ_+ and Δ_- are the same, and the corresponding solution will be $E = \pm\Delta_+$. However, these solutions do not correspond to an edge state since $\kappa_\pm = 0$. Therefore, there is no midgap edge bound state [7] for equal or larger singlet component compared to the triplet component.

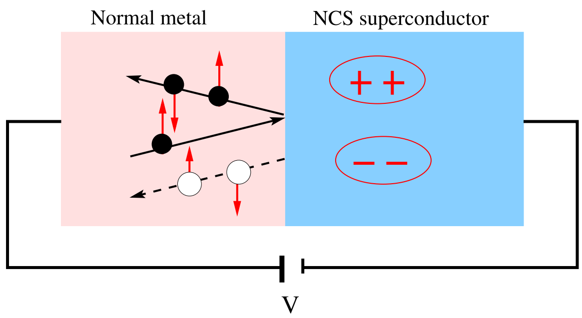

Figure 2. A schematic diagram of tunneling from a normal metal to an NCS superconductor. Up (or down) spin electrons (filled circle) incident on the junction from the normal metal side get partly reflected as both spin-up and spin-down electrons as well as holes (open circle) in the Andreev process making Cooper pairs inside the NCS superconductor at both positive and negative helicity bands. A bias voltage V may be applied across the junction.

3. Charge and spin tunneling conductance

Consider a junction between a ballistic normal (at $x < 0$) metal and an NCS (at $x > 0$) superconductor. The junction is characterized by an insulating barrier at $x = 0$ with a delta-function potential $V(x) = U\delta(x)$. The Hamiltonian for the normal metal is $H_N = \xi_{\mathbf{k}}\,\hat{1}$. In this geometry, the wavefunction for an electron with spin σ (numerically $\pm$ and symbolically $\uparrow$ or $\downarrow$ respectively) incident from the normal metal on the junction is given by

$$\Psi_N^\sigma(x, y) = \mathrm{e}^{\mathrm{i}k_y y}[(\psi_e^\sigma + a_{\sigma,\sigma}\psi_h^\sigma + a_{\sigma,-\sigma}\psi_h^{-\sigma})\mathrm{e}^{\mathrm{i}k_{Fx}x} + (b_{\sigma,\sigma} + b_{\sigma,-\sigma})\psi_e^\sigma\mathrm{e}^{-\mathrm{i}k_{Fx}x}] \qquad (9)$$

within the 'Andreev approximation', where ${}^{\mathrm{T}}\psi_e^\uparrow = (1, 0, 0, 0)$, ${}^{\mathrm{T}}\psi_e^\downarrow = (0, 1, 0, 0)$, ${}^{\mathrm{T}}\psi_h^\uparrow = (0, 0, 1, 0)$, ${}^{\mathrm{T}}\psi_h^\downarrow = (0, 0, 0, 1)$, and $k_{Fx} = \sqrt{k_F^2 - k_y^2}$ with Fermi momentum k_F in the normal metal. Here $a_{\sigma,\sigma}$, $a_{\sigma,-\sigma}$ $b_{\sigma,\sigma}$, and $b_{\sigma,-\sigma}$ are the parallel-spin Andreev, antiparallel-spin Andreev, parallel-spin normal, and antiparallel-spin normal reflection coefficients respectively. The normal and Andreev reflection processes and formation of Cooper pairs inside the superconductor are schematically shown in figure 2.

The angle resolved charge and spin tunneling conductances are thus defined to be [14, 15]

$$g_c(\phi) = \left(1 + \frac{1}{2}\sum_\sigma[|a_{\sigma,\sigma}|^2 + |a_{\sigma,-\sigma}|^2 - |b_{\sigma,\sigma}|^2 - |b_{\sigma,-\sigma}|^2]\right)\cos\phi, \qquad (10)$$

$$g_s(\phi) = \left(\frac{1}{2}\sum_\sigma \sigma[|a_{\sigma,\sigma}|^2 - |a_{\sigma,-\sigma}|^2 - |b_{\sigma,\sigma}|^2 + |b_{\sigma,-\sigma}|^2]\right)\cos\phi \qquad (11)$$

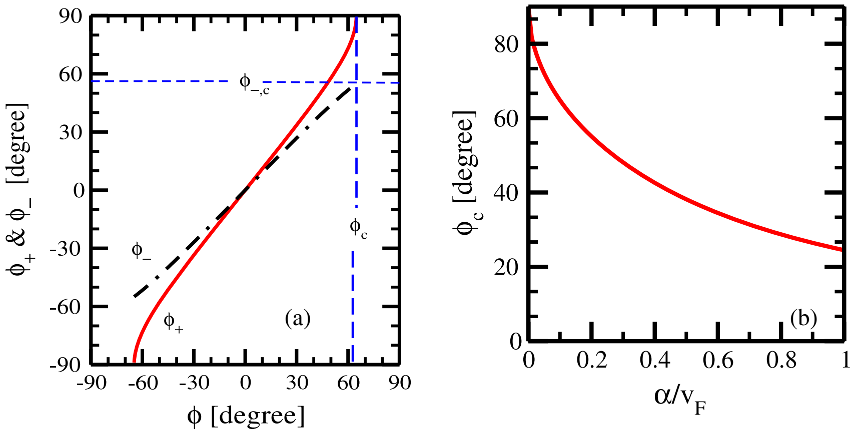

Figure 3. (a) Variation of the angles ϕ_+ and ϕ_- with the angle of incidence ϕ for $\alpha/v_F = 0.1$. The critical angle ϕ_c and correspondingly the critical angle for negative helicity band, denoted as $\phi_{c,-}$ are shown. (b) Variation of ϕ_c against α/v_F.

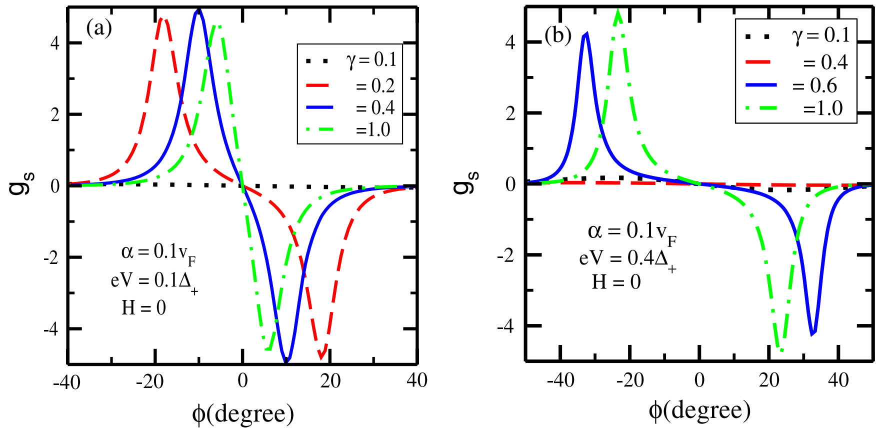

Figure 4. The variation of spin conductance g_s (in the unit of G_{nc}) with the incident angle ϕ for different values of γ at quasiparticle energy $E = eV = 0.1\Delta_+$ (a) and $0.4\Delta_+$ (b) for $H = 0$, $Z = 5$, and $\alpha = 0.1v_F$.

respectively at zero temperature. Here the angle ϕ is defined as $k_y = k_F \sin\phi$. The reflection amplitudes can be found by matching the wavefunctions and the velocity flux at $x = 0$:

$$\Psi_N^\sigma(x = 0, y) = \Psi_S(x = 0, y), \tag{12}$$

$$\begin{pmatrix} -\frac{i}{m}\partial_x & 0 & 0 & 0 \\ 0 & -\frac{i}{m}\partial_x & 0 & 0 \\ 0 & 0 & \frac{i}{m}\partial_x & 0 \\ 0 & 0 & 0 & \frac{i}{m}\partial_x \end{pmatrix} \Psi_N^\sigma(x, y)|_{x=0}$$
$$= \begin{pmatrix} -\frac{i}{m}\partial_x & i\alpha & -i\frac{\Delta_t}{k_F} & 0 \\ -i\alpha & -\frac{i}{m}\partial_x & 0 & -i\frac{\Delta_t}{k_F} \\ i\frac{\Delta_t}{k_F} & 0 & \frac{i}{m}\partial_x & -i\alpha \\ 0 & i\frac{\Delta_t}{k_F} & i\alpha & \frac{i}{m}\partial_x \end{pmatrix} \Psi_S(x, y)|_{x=0}$$
$$+ 2iU \begin{pmatrix} 1 & 0 & 0 & 0 \\ 0 & 1 & 0 & 0 \\ 0 & 0 & -1 & 0 \\ 0 & 0 & 0 & -1 \end{pmatrix} \Psi_N^\sigma(x = 0, y). \tag{13}$$

For nonzero α, the phase space of the incident electron that takes place in Andreev reflection gets restricted. The angles of $\boldsymbol{k}$ in the two bands inside the NCS superconductor is restricted by $-\frac{\pi}{2} \leqslant \phi_\pm \leqslant \frac{\pi}{2}$. The conservation of momentum implies $k_F \sin\phi = k_F^+ \sin\phi_+ = k_F^- \sin\phi_-$. The variation of $\phi_\pm$ with the incident angle ϕ is shown in figure 3(a) for $\alpha/v_F = 0.1$. It is clear that $-\phi_c \leqslant \phi \leqslant \phi_c$, where ϕ_c is the critical angle of incidence beyond which the incident electron becomes totally reflected. This critical angle corresponds to $\phi_+ = \pi/2$ and $\phi_- = \phi_{-,c}$. The angle ϕ_c decreases with the increase of α as shown in figure 3(b). The total charge and spin tunneling conductances in the unit of normal tunneling charge conductance G_{nc} become

$$G_c = \frac{1}{G_{nc}} \int_{-\phi_c}^{\phi_c} g_c(\phi)\, d\phi; \qquad G_s = \frac{1}{G_{nc}} \int_{-\phi_c}^{\phi_c} g_s(\phi)\, d\phi. \tag{14}$$

We then consider the application of a magnetic field H perpendicular to the plane of the NCS superconductor. Assuming the penetration depth is much larger than the coherence length of the superconductor, the corresponding vector potential in the Landau gauge may be approximated as $\boldsymbol{A}(\boldsymbol{r}) = (0, -H\lambda_d \exp(-x/\lambda_d), 0)$ with the penetration depth λ_d. In a semiclassical approximation where the quantization of the Landau level may be neglected, the quasiparticle energy becomes Doppler shifted [17]: $E \to E - H\Delta_+ \sin\phi/H_0$ with a characteristic field $H_0 = \Phi_0/(\pi^2\xi\lambda_d)$, where the coherence

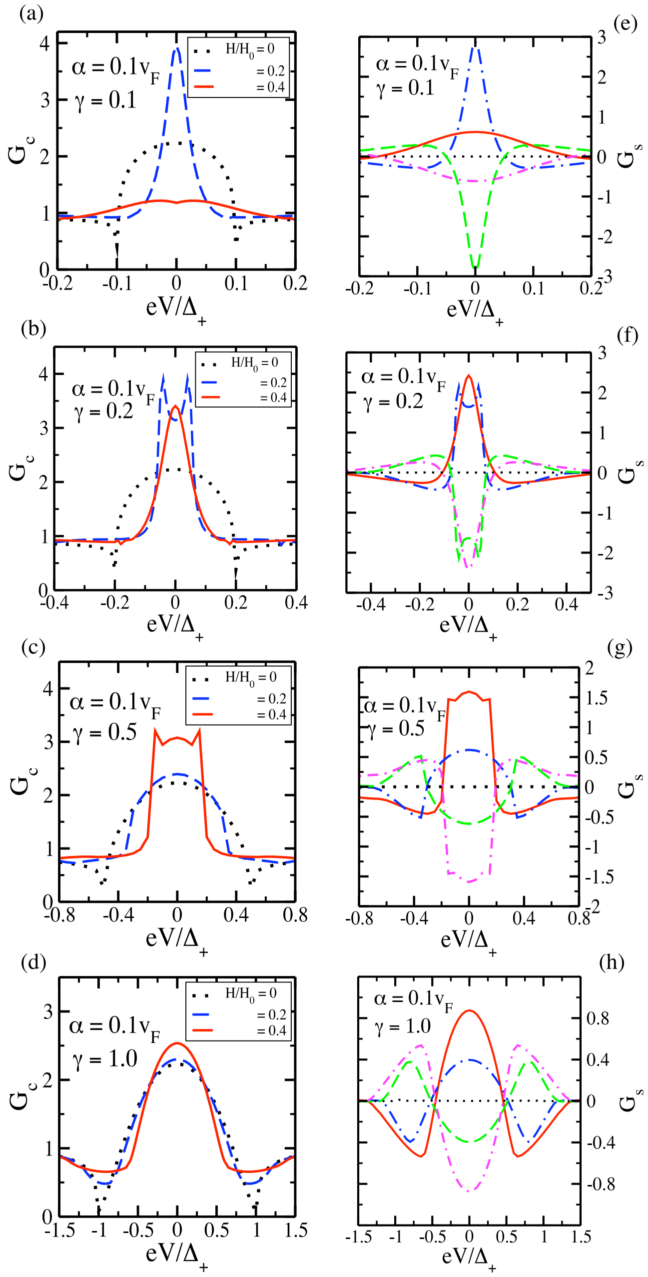

Figure 5. The variation of charge conductance (a)–(d) and spin conductance (e)–(h) with bias energy eV. The parameters $Z = 5$, $\gamma = 0.1$ (a), (e), 0.2 (b), (f), 0.5 (c), (g), and 1.0 (d), (h), and $\alpha/v_F = 0.1$ are chosen. The magnetic filed H/H_0 chosen for the panels (e)–(h) are -0.4 (solid line), -0.2 (dot and long-dashed line), 0 (dotted line), 0.2 (dashed line), and 0.4 (dot and short-dashed line).

length $\xi = k_F/(\pi m \Delta_+)$ (as Δ_+ is larger among two pair amplitudes) and Φ_0 is the flux quantum. The Zeeman coupling may be neglected since the energy of Doppler shift energy is very high compared to the Zeeman energy for large λ_d. In contrast, the Zeeman energy is responsible for breaking the degeneracy between the helical edge modes in quantum spin Hall systems (QSHS) [21–23] and it modulates the transport properties. The modulation of the spin conductance with H due to the Doppler shift in NCS superconductor is the superconducting analogue [7] to the QSHS as a topological system.

In the presence of small magnetic field, where the formation of Landau levels are ignored, the wavefunction in the normal side remain as a superposition of plane waves as in the case of zero magnetic field. We also ignore the spin reflection asymmetry arising from Zeeman coupling in the normal side. We numerically evaluate the coefficients as and bs, both in the absence and presence of magnetic field, using equations (12) and (13) and plug them into equations (10) and (11) to determine the angle resolved charge and spin conductances. The total charge and spin conductances are then evaluated using equation (14). The numerical results are presented below for a fixed parameter $Z = 2U/v_F$ characterizing the effective strength of the barrier. However, the qualitative behavior is independent of Z as we see below.

4. Results

Although the NCS superconductors do not break time reversal symmetry, the angle resolved spin conductance is nonvanishing and $g_s(\phi)$ shows peaks at those values of ϕ for which the energy of the incident electron matches with the energy of the midgap edge state. The large $g_s(\phi)$ is due to the presence of helical edge modes [7] in NCS superconductors. We have found that $g_s(\phi)$ depends very weakly on α/v_F around the peak position. The variation of $g_s(\phi)$ is shown in figure 4 for different values of the ratio $\gamma = \Delta_-/\Delta_+$, and two different values of quasiparticle energy eV for a bias voltage V across the junction. The peak in $g_s(\phi)$ is present for $|eV| < \Delta_-$. The peak shifts towards smaller $|\phi|$ for larger values of γ. However, the total spin conductance becomes zero since $g_s(\phi) = -g_s(-\phi)$ for any values of α/v_F, γ, and eV.

The total charge and spin conductances for different values of H and γ are shown in figure 5. Since G_c and G_s are weakly dependent on α, we choose a fixed value $\alpha/v_F = 0.1$. The charge conductance is minimum at $|eV| = \Delta_-$ in the absence of magnetic field since Δ_- is the lowest energy scale in the bulk superconductor. The zero bias peak in G_c at $H = 0$ is present as is observed [16–18] in d-wave and predicted [19, 20] in p-wave superconductors. When the bound state quasiparticle energy $E = \Delta_-$, $\phi = \phi_c$. In that case $\gamma = |eV \pm \frac{H}{H_0}\sin\phi_c|$ in the presence of bias and magnetic field. The zero bias peak remains for $\frac{|H|}{H_0} > \frac{\gamma}{\sin\phi_c}$, but G_c decreases with the increase of H at high magnetic field. The ZBP in G_c at finite magnetic field splits into two sharp peaks at finite bias (one at negative bias and the other at positive bias) and a dip in zero bias, when $\gamma > \frac{|H|}{H_0}\sin\phi_c$. The peaks shift towards higher $|eV|$ and becomes weaker on lowering $|H|$ so that the ZBP reappears again at a low field. Although the total spin conductance G_s is zero at any bias, it modulates with eV at finite H. It has the symmetry: $G_s(eV, H) = -G_s(eV, -H) = -G_s(-eV, H)$. The disappearance and reappearance of ZBP in the magnitude of G_s, and the splitting of ZBP at finite magnetic field, is similar to that of G_c.

The ZBP in G_c increases initially with the magnetic field and it subsequently decreases creating a peak at $|H| \sim \gamma H_0$, i.e., when all the midgap edge states up to the energy Δ_- take part in the conduction process. Likewise ZBP in G_s also behave the same way with the important exception that the

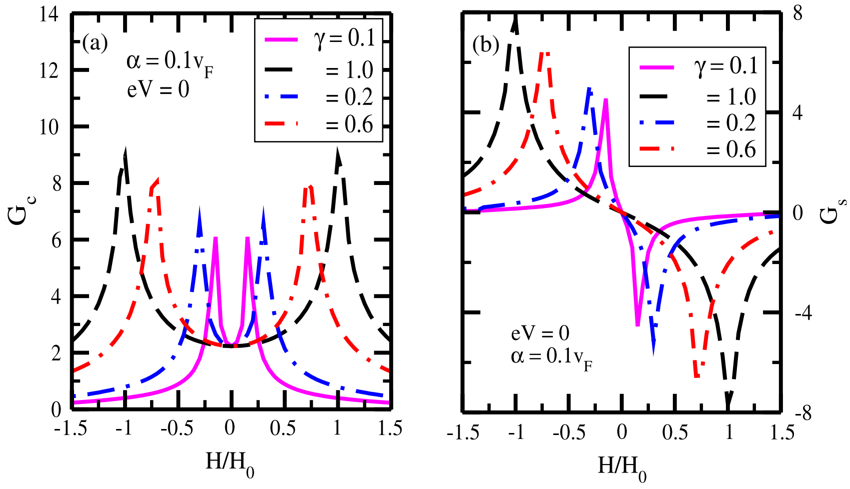

Figure 6. (a) Charge conductance and (b) spin conductance versus H/H_0 for $Z = 5$, $\alpha/V_F = 0.1$ and at zero bias. The curves from the left correspond to $\gamma = 1.0$, 0.6, 0.2, and 0.1.

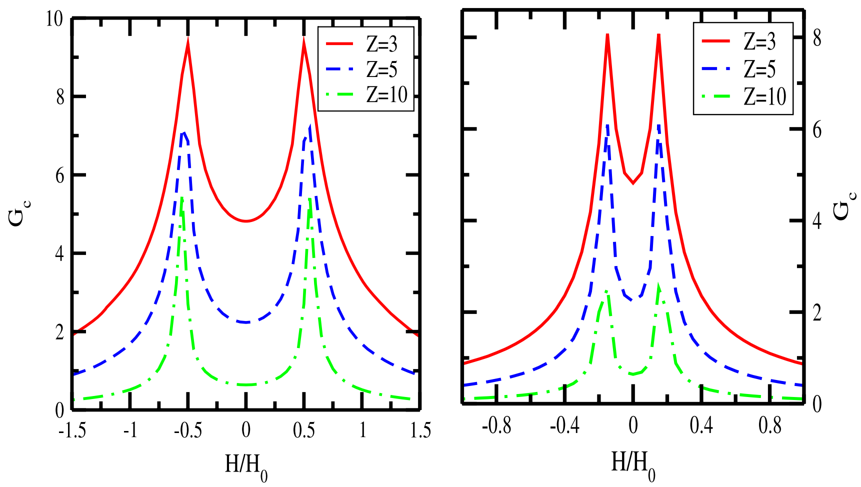

Figure 7. Variation of zero bias charge conductance with H at barrier heights $Z = 3$, 5, and 10 with $\gamma = 0.4$ (left panel) and 0.1 (right panel) when $\alpha/V_F = 0.1$.

latter changes sign on reversing the magnetic field direction, although G_s is zero at $H = 0$. This has an extraordinary effect on the spin as well as charge conductances, as shown in figure 6, by the presence of midgap helical edge states. We observe that the value of $|H|/H_0$ at which the peaks occur decreases with γ, since Δ_- decreases with a fixed Δ_+. For $\gamma = 1$, the ZBP in G_c is almost constant at small $H(|H| < 0.5H_0)$ but the ZBP in G_s changes sharply at small H, as was obtained by Tanaka *et al* [7]. However when γ is small, the ZBP in both G_c and G_s form peaks at a much smaller field. In a system like Li_2Pt_3B [2], the spin triplet and singlet components are of the same order, which means γ is small and it is estimated to be $\sim$0.24. Therefore in such systems the presence of helical edge states will be revealed in the form of peaks for zero bias charge and spin magneto-tunneling-conductance at as small a magnetic field as $\sim 0.35H_0 \sim 0.07$ T for typical values of $\xi \sim 10$ nm and $\lambda_d \sim 100$ nm.

In our study so far, we have chosen $Z = 5$ as the parameter for the barrier height. Figure 7 shows the variation of G_c at zero bias as a function of magnetic field for different values of Z and γ. We notice that the qualitative behavior, in particular the positions of ZBP are independent of Z. The values of the tunneling conductances increase with decreasing Z, as expected.

5. Summary

To summarize, helical edge states [7] exist in a noncentrosymmetric superconductor provided the triplet-pair-amplitude is larger than the singlet-pair-amplitude, i.e., when $0 < \gamma \leqslant 1$. The energies of the midgap ($E < \Delta_-$) edge states decrease with γ. We have studied the consequence of these edge states on the charge and spin tunneling conductances from a normal metal to a noncentrosymmetric superconductor. The angle resolved spin conductance g_s shows a peak at an angle that corresponds to the conduction through the edge state. The g_s show peaks when the bias energy $|eV| < \Delta_-$. It changes sign on the reversal of sign of the angle since the conduction is due to helical edge states and this change of sign leads to a zero total spin conductance G_s irrespective of the bias. However, the Doppler shifted energy of the quasiparticles for the application of H leads to nonzero G_s and it modulates with eV for different magnetic fields. The zero bias peak is present at high H (although G_s vanishes at very high H). This peak splits into two (one at positive bias and the other at negative bias) and a dip is formed at zero bias on reduction of the field. The double peaks occur when $\gamma > \frac{|H|}{H_0} \sin\phi_c$ and they become weaker on lowering the field so that a zero bias peak reappears at very low field. Similarly, the disappearance and reappearance of zero bias peak in total charge conductance G_c also occur. Moreover, G_c has a dip at $|eV| = \Delta_-$. Interestingly, the magnitude of zero bias charge as well as spin magneto-tunneling-conductance increases with $|H|$, and form peaks at $|H| \sim \gamma H_0$, i.e., when all the midgap helical edge states take part in the conduction process.

Acknowledgment

SPM is supported by CSIR, Government of India.

References

[1] Bauer E, Hilscher G, Michor H, Paul C, Scheidt E W, Gribanov A, Seropegin Y, Noel H, Sigrist M and Rogl P 2004 *Phys. Rev. Lett.* **92** 027003
[2] Yuan H Q, Agterberg D F, Hayashi N, Badica P, Vandervelde D, Togano K, Sigrist M and Salamon M B 2006 *Phys. Rev. Lett.* **97** 017006
[3] Reyren N, Thiel S, Caviglia A D, Kourkoutis L F, Hammerl G, Richter C, Schneider C W, Kopp T, Ruetschi A S, Jaccard D, Gabay M, Muller D A, Triscone J M and Mannhart J 2007 *Science* **317** 1196
[4] Frigeri P A, Agterberg D F, Koga A and Sigrist M 2004 *Phys. Rev. Lett.* **92** 097001
Frigeri P A, Agterberg D F, Koga A and Sigrist M 2004 *Phys. Rev. Lett.* **93** 099903(E) (erratum)
[5] Mandal S S and Mukherjee S P 2006 *J. Phys.: Condens. Matter* **18** L593
[6] Andreev A F 1964 *Sov. Phys.—JETP* **19** 1228
[7] Tanaka Y, Yokoyama T, Balatsky A V and Nagaosa N 2009 *Phys. Rev.* B **79** 060505(R)
[8] Vorontsov A B, Vekhter I and Eschrig M 2008 *Phys. Rev. Lett.* **101** 127003
[9] Read N and Green D 2000 *Phys. Rev.* B **61** 10267
[10] Sato M and Fujimoto S 2009 *Phys. Rev.* B **79** 094504
[11] Stone M and Roy R 2004 *Phys. Rev.* B **69** 184511
[12] Luke G M, Fudamoto Y, Kojima K M, Larkin M I, Merrin J, Nachumi B, Uemura Y J, Maeno Y, Mao Z Q, Mori Y, Nakamura H and Sigrist M 1998 *Nature* **394** 558
[13] Rashba E I 1960 *Sov. Phys.—Solid State* **2** 1109
[14] Blonder G E, Tinkham M and Klapwijk T M 1982 *Phys. Rev.* B **25** 4515
[15] Kashiwaya S, Tanaka Y, Yoshida N and Beasley M R 1999 *Phys. Rev.* B **60** 3572
[16] Covington M, Aprili M, Paraoamu E and Green L H 1997 *Phys. Rev. Lett.* **79** 277
[17] Fogelstrom M, Rainer D and Sauls J A 1997 *Phys. Rev. Lett.* **79** 281
[18] Aprili M, Badica E and Greene L H 1999 *Phys. Rev. Lett.* **83** 4630
[19] Yokoyama T, Iniotakis C, Tanaka Y and Sigrist M 2008 *Phys. Rev. Lett.* **100** 177002
[20] Tanaka Y, Tanuma Y, Kuroki K and Kashiwaya S 2002 *J. Phys. Soc. Japan* **71** 2102
[21] Kane C L and Mele E J 2005 *Phys. Rev. Lett.* **95** 146802
Kane C L and Mele E J 2005 *Phys. Rev. Lett.* **95** 226801
[22] Bernevig B A, Huges T L and Zhang S C 2006 *Science* **314** 1757
[23] Konig M, Wiedmann S, Brune C, Roth A, Buhmann H, Molenkamp L, Qi X L and Zhang S C 2007 *Science* **318** 766